Mapping Region-Specific Longitudinal Cortical Surface Expansion from Birth to 2 Years of Age

Gang Li[1], Jingxin Nie[1], Li Wang[1], Feng Shi[1], Weili Lin[1], John H. Gilmore[2] and Dinggang Shen[1]

[1]Department of Radiology and BRIC and [2]Department of Psychiatry, University of North Carolina at Chapel Hill, NC, USA

Address correspondence to Dinggang Shen, Radiology and BRIC, UNC-CH School of Medicine, MRI Building, CB #7513, 106 Mason Farm Road, Chapel Hill, NC 27599, USA. E-mail: dinggang_shen@med.unc.edu

The human cerebral cortex develops rapidly and dynamically in the first 2 years of life. It has been shown that cortical surface expansion from term infant to adult is highly nonuniform in a cross-sectional study. However, little is known about the longitudinal cortical surface expansion during early postnatal stages. In this article, we generate the first longitudinal surface-based atlases of human cortical structures at 0, 1, and 2 years of age from 73 healthy subjects. On the basis of the surface-based atlases, we study the longitudinal cortical surface expansion in the first 2 years of life and find that cortical surface expansion is age related and region specific. In the first year, cortical surface expands dramatically, with an average expansion of 1.80 times. In particular, regions of superior and medial temporal, superior parietal, medial orbitofrontal, lateral anterior prefrontal, occipital cortices, and postcentral gyrus expand relatively larger than other regions. In the second year, cortical surface still expands substantially, with an average expansion of 1.20 times. In particular, regions of superior and middle frontal, orbitofrontal, inferior temporal, inferior parietal, and superior parietal cortices expand relatively larger than other regions. These region-specific patterns of cortical surface expansion are related to cognitive and functional development at these stages.

Keywords: cortical surface expansion, longitudinal cortical development, longitudinal surface-based atlas, infant cortical folding

Introduction

The adult human cerebral cortex is a highly convoluted and variable structure composed of sulci and gyri (Ono et al. 1990), which emerge in late gestation (Retzius 1890; Chi et al. 1977; Dubois et al. 2008). At term birth, all major sulci and gyri have been well established (Chi et al. 1977), although both brain volume and cortical surface area are only one-third of those of adults (Thompson et al. 2007; Hill, Dierker et al. 2010). After birth, tertiary folding structures are still undergoing development (Chi et al. 1977; Ono et al. 1990; Armstrong et al. 1995; Toro and Burnod 2005; Nie, Li et al. 2011), in concert with the rapid development of related cognitive and motor functions (Gilmore et al. 2007). Understanding normal cortical surface development in the early postnatal period would provide important insight into neurodevelopmental disorders (Gilmore et al. 2007).

Owing to the cellular nonuniformities, it is anticipated that there would be regional differences in macroscopic aspects of postnatal cortical development (Hill, Inder et al. 2010). Hill et al. (Hill, Inder et al. 2010) generated the first surface-based atlas of cortical structures of term-born infants using a small population of 12 healthy subjects. On the basis of the atlas, they compared the cortical surfaces of the 12 infants and 12 adults cross-sectionally to demonstrate the highly nonuniform postnatal cortical surface expansion, with the lateral temporal, parietal, and frontal regions expanding nearly twice as much as other regions in the insular and medial occipital cortex (Hill, Inder et al. 2010). However, cross-sectional studies are likely affected by variations of intersubjects and cohort effects (Gogtay et al. 2004), and to date the longitudinal cortical surface expansion in the early postnatal stage still remains largely unknown. In this article, we constructed the first longitudinal surface-based atlases of human cortical structures at birth, 1 year of age, and 2 year of age from a population of 73 healthy subjects. The surface-based atlases were generated by the landmark-free groupwise registration of cortical surfaces; thus, the generated atlas is unbiased to any individual and can also capture the variability of cortical folding. We then used the longitudinal surface-based atlases to study the longitudinal cortical surface expansion in the first 2 years of life. We find that cortical surface expansion is both age related and region specific. In the first year, the cortical surface area expands dramatically, with an average expansion of 1.80 times. Specifically, regions of superior and medial temporal, superior parietal, medial orbitofrontal, lateral anterior prefrontal cortices, postcentral gyri, and occipital lobes on both hemispheres expand relatively larger than other cortical regions. In the second year, cortical surface area expansion is still substantial, with an average expansion of 1.20 times. Regions of superior and middle frontal, orbitofrontal, inferior temporal, inferior parietal, and superior parietal cortices in both hemispheres expand relatively larger than other cortical regions. The region-specific patterns of cortical surface area expansion in the first and the second year are related to the cognitive and functional development at different stages.

Materials and Methods

Subjects

This study was approved by the Institutional Review Board of the University of North Carolina (UNC) School of Medicine. The parents were recruited during the second trimester of pregnancy from the UNC hospitals and written informed consent forms were obtained from all the parents. The presence of abnormalities on fetal ultrasound, or major medical or psychotic illness in the mother, was taken as exclusion criteria. The infants were free of congenital anomalies, metabolic disease, and focal lesions. None of the subjects was sedated for MRI. Before the subjects were imaged, they were fed, swaddled, and fitted with ear protection (Gilmore et al. 2011).

Complete 0-1-2 data of 73 normal infants was acquired in 30 singletons (20 males/10 females) and 43 twins (22 males/21 females; 7 monozygotic twin pairs, 10 dizygotic pairs, and 8 "single" twins). The mean gestational age at birth was 37.9 ± 1.6 weeks. The mean ages at the scan are 25.5 ± 10.8 days, 392.8 ± 22.1 days, and 758 ± 38.1 days, respectively. This same dataset has been used in a prior study of development of cortical gray matter volume (Gilmore et al. 2011).

MR Image Acquisition

Images were acquired on a Siemens head-only 3T scanner (Allegra, Siemens Medical System, Erlangen, Germany) with a circular polarized head coil. For T_1-weighted images, 160 sagittal slices were obtained by using the 3D magnetization-prepared rapid gradient echo sequence: TR = 1900 ms, TE = 4.38 ms, inversion time = 1100 ms, Flip Angle = 7°, and resolution = $1 \times 1 \times 1$ mm^3. For T_2-weighted images, 70 transverse slices were acquired with turbo spin-echo sequences: TR = 7380 ms, TE = 119 ms, Flip Angle = 150°, and resolution = $1.25 \times 1.25 \times 1.95$ mm^3 (Gilmore et al. 2011). Data were collected longitudinally at 3 age groups: neonates, 1 year of age, and 2 year of age. Data with motion artifacts was discarded and a rescan was made when possible. The variation of age at MRI for each scan is relatively small, and the population can be divided into age groups concentrated around 0, 1, and 2 years of age.

Image Processing

Before tissue segmentation and cortical surface reconstruction, all images were preprocessed using the following procedure. Noncerebral tissues were stripped by (Shi et al. 2012), followed by manual editing with ITK-SNAP software (Yushkevich et al. 2006) to ensure accurate skull removal. Cerebellum and brain stem are removed by in-house developed tools. Intensity inhomogeneity correction was performed with N3 method (Sled et al. 1998) to alleviate the influence on subsequent tissue segmentation. All images at each age were rigidly aligned to the age-matched infant image intensity atlas (Shi et al. 2011). Because of the low tissue contrast and difference in cortical shapes compared with adults, tissue segmentation methods developed for adult brain MR images do not work well on the infant brain MR images (Hill, Dierker et al. 2010). Therefore, tissue segmentation of infant brain MR images were performed by a dedicated longitudinally guided level-set–based method (Wang et al. 2011) by combining local intensity information, atlas spatial prior, cortical thickness constraint, and longitudinal information by longitudinal image registration (Shen and Davatzikos 2004; Xue et al. 2006) into a variational framework. Figure 1.1*a,b,c* shows a T_2-weighted MR image at birth, corresponding skull-stripping result, and tissue segmentation result, respectively. After tissue segmentation, the lateral ventricles and subcortical structures were masked and filled, and then each brain was separated into left and right hemispheres as shown in Figure 1.1(*d*).

Cortical Surface Reconstruction

The inner cortical surface (the interface between white matter and gray matter) was obtained by correcting the topological defects (Fischl et al. 2001; Shattuck and Leahy 2002) and tessellating the white matter as a triangular mesh to ensure a spherical topology for each hemisphere. Since the transient subplate zone, which is interposed between the immature cortical plate and white matter, might still exist after birth, the inner cortical surface at birth was defined as the interface between the cortex plate and white matter zone (including white matter and transient subplate zone) (Nie, Li et al. 2011). The inner cortical surface was then deformed by preserving its initial topology for reconstruction of the central cortical surface (Li et al. 2012), which was defined as the layer lying in the geometric center of the cortex and approximately corresponding to the cytoarchitectonic layer 4 (Xu et al. 1999; Van Essen 2005; Liu et al. 2008). The central cortical surface was adopted for performing analysis of the cortical surface expansion as did in (Hill, Inder et al. 2010), since it provided a more balanced representation of gyral and sulcal regions (Van Essen 2005). The inner cortical surface, which had vertex-to-vertex correspondences with the central cortical surface, was further smoothed, inflated, and mapped to a standard sphere by minimizing the metric distortion between the cortical and the spherical representation (Fischl, Sereno, Dale 1999). Figure 1.1*e,f,g,h* shows an example of the reconstructed inner cortical surface, central cortical surface, the inflated inner cortical surface, and the spherical representation of the inner cortical surface, respectively. Note that the inflated cortical surface and the spherical representation are color-coded by the average convexity of the cortical surface, which integrates the normal movement of a vertex during cortical surface inflation and reflects the large-scale geometry of the cortical surface (Fischl, Sereno, Tootell et al. 1999). Figures 1.2 shows the longitudinal inner cortical surfaces (color-coded by mean curvatures) of a typical subject at 0, 1, and 2 years of age. Generally, gyri have negative mean curvatures, and sulci have positive mean curvatures (Note that we here adopt the inward-oriented normal vector field). As we can see, the major cortical folding of sulci and gyri has been well developed at term birth, and is well preserved during the cortical development from 0 to 2 years of age.

Surface-Based Atlas Generation

To build the longitudinal surface-based atlases of cortical structures, we need to determine the longitudinal vertex-to-vertex correspondences of cortical surfaces at different ages of each subject and also the cross-sectional vertex-to-vertex correspondences of cortical surfaces between different subjects at each age. To establish longitudinal vertex-to-vertex correspondences of cortical surfaces at different ages, for each hemisphere of each subject, the cortical surface at 0-year of age was registered to the corresponding cortical surface at 1-year of age using Spherical Demons registration method (Yeo et al. 2010). Spherical Demons aligns the cortical folding patterns mapped in the spherical space based on several geometric features of cortical surfaces, including mean curvature of the inflated cortical surface, average convexity of the cortical surface, and mean curvature of the cortical surface. It has been shown that the Spherical Demons achieved similar registration accuracy as FreeSurfer, but with much faster computational speed (Yeo et al. 2010). Similarly, the cortical surface of each hemisphere of each subject at 1-year of age was registered to the corresponding cortical surface at 2 years of age. The deformation map from 0 to 2 years of age of each hemisphere of each subject was obtained by concatenating the 2 deformation maps from 0- to 1-year of age and from 1 to 2 years of age by using the method in (Van Essen et al. 2011). In the next step, we focus on estimating atlases at different ages, and then build their relative deformation maps. The surface-based atlas of cortical structures at each age of each hemisphere was constructed by groupwise registration of cortical surfaces of all subjects at the age using Spherical Demons. Thus, the surface-based atlases are unbiased to any individual and can capture the variability of cortical folding. Specifically, at each age, first, an atlas consisting of the mean and variance of cortical geometry of all subjects was computed; second, all cortical surfaces were registered to the computed atlas; and finally, the atlas was updated based on the current registration results. The registration and atlas updating were iteratively performed. In our application, 3 iterations of registration were performed and reasonable results were achieved. On the other hand, to compute the deformation map between any 2 atlases (at 2 different ages), the longitudinal deformation of each subject projected in the respective atlas spaces of the ith and the jth year(s) $(i, j \in 0, 1, 2, i < j)$ was first obtained by concatenating 3 deformation maps: deformation from the atlas at the ith year to the cortical surface at the ith year, longitudinal deformation from the cortical surface at the ith year to the cortical surface at the jth year(s), and deformation from the cortical surface at the jth year(s) to the atlas at the jth year (s). The deformation map between any 2 atlases was thus obtained by averaging longitudinal deformations projected in the 2 atlas spaces of all subjects. Figure 1.3 illustrates the flowchart of generating longitudinal surface-based atlases of cortical structures at 0, 1, and 2 years of age.

Computing Cortical Surface Area Expansion

After building the longitudinal surface-based atlases, the central cortical surface of each hemisphere of each subject at 2 years of age was resampled to a standard-mesh tessellation with 163 842 vertices based on deformation from the surface-based atlas at 2 years of age to the individual cortical surface, thus establishing the vertex-to-vertex correspondences at each hemisphere across all subjects at 2 years of age. Based on the longitudinal registration result of each subject, the standard-mesh tessellation of each subject at 2 years of age was warped to 1-year of age and 0-year of age, respectively, thereby establishing the longitudinal vertex-to-vertex correspondences of each
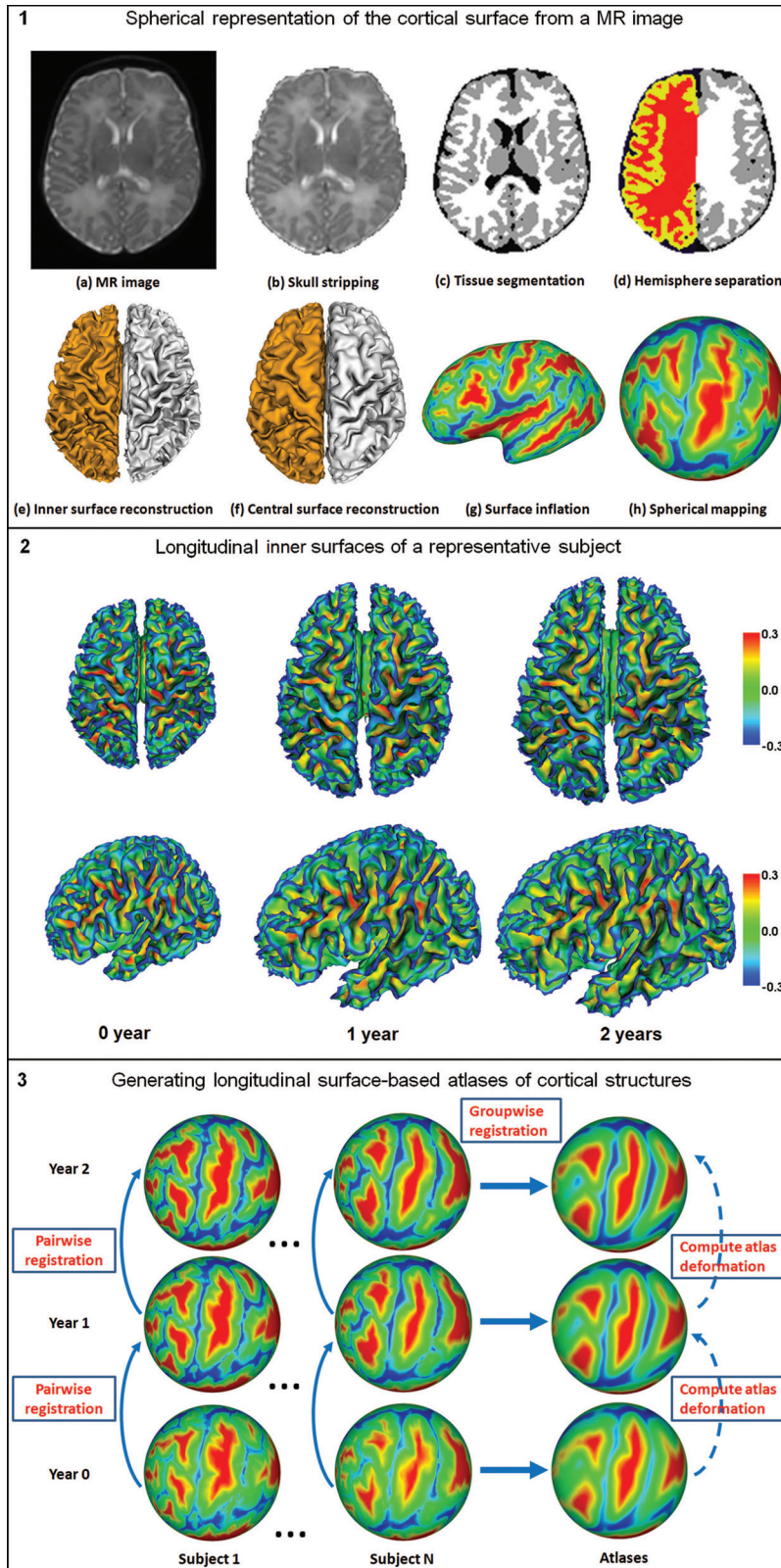
Figure 1. Illustration of cortical surface reconstruction and longitudinal surface-based atlases generation.

subject. Note that the occupied area of each vertex was computed as one-third the sum of areas of all triangles associated with that vertex. And the fractional area of each vertex was computed as the occupied area of each vertex as the fraction of the total surface area. The cortical surface area expansion map from the ith to the jth year(s) old $(i, j, \in 0, 1, 2, i < j)$ of each hemisphere of each subject was computed by comparing the occupied vertex area at each vertex at the jth year(s) to that of its corresponding vertex at the ith year. The surface areal expansion map of each hemisphere of each subject was smoothed by using an iterative nearest neighbor-averaging procedure
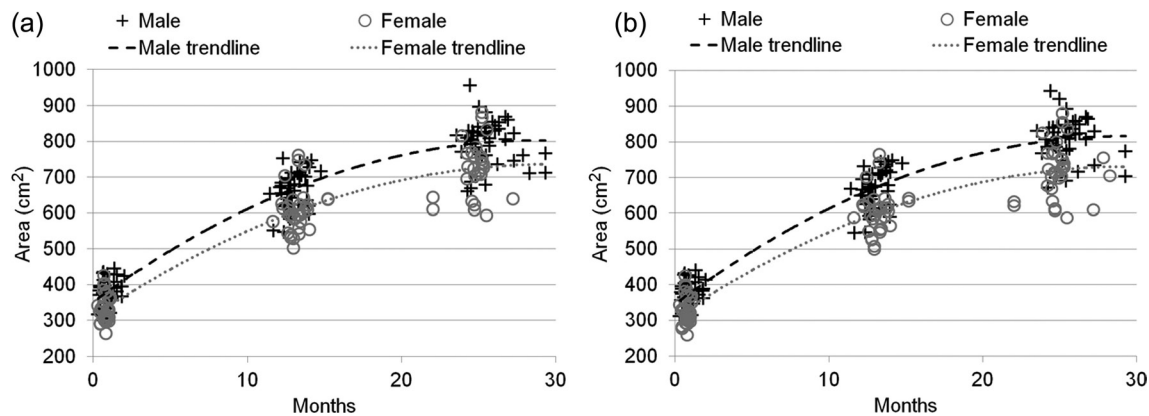
Figure 2. The respective distribution of longitudinal cortical surface areas of 73 subjects at 0, 1, and 2 years of age. The results on both (a) left and (b) right hemispheres are provided.

Table 1

The mean and standard deviation of longitudinal cortical surface areas of the 73 subjects at 0, 1 and 2 years of age, respectively

Subjects	0-year-old surface area (cm²)		1-year-old surface area (cm²)		2-year-old surface area (cm²)	
	Left	Right	Left	Right	Left	Right
All (n = 73)	361 ± 43	356 ± 43	640 ± 63	641 ± 65	770 ± 77	771 ± 80
Male (n = 42)	381 ± 34	375 ± 35	666 ± 52	669 ± 54	806 ± 57	809 ± 59
Female (n = 31)	333 ± 39	330 ± 40	603 ± 58	603 ± 60	721 ± 73	719 ± 75

on the surface mesh (Han et al. 2006). All smoothed surface areal expansion maps were generated by 40 iterations of smoothing, approximately corresponding to 5 mm Gaussian smoothing kernel (Han et al. 2006). The smoothed surface areal expansion maps of all subjects are averaged to generate the final surface areal expansion map.

Results

Global Cortical Surface Area Expansion in the First 2 Years

Figure 2 shows the distribution of cortical surface areas of the 73 subjects at 0, 1, and 2 years of age, and Table 1 provides the mean and standard deviation of cortical surface areas of the 73 subjects. Note that all the cortical surface areas were measured in their native space. The cortical surface area of male is generally larger than that of female at each age, consistent to the findings with the brain volume of male being larger than that of female (Shi et al. 2011). Specifically, the cortical surface area is about 14%, 11%, and 12% lager in males compared with females at 0, 1, and 2 years of age, respectively, consistent to the findings that the cortical surface area is about 10% lager in males compared with females in adults (Van Essen et al. 2011). However, this is different from another study with a smaller sample size, which found no gender difference in infants (Hill, Dierker et al. 2010). By using the unpaired t-test, it is found that the cortical surface area of male is statistically larger than that of female on both hemispheres of all 3 ages, with the P value consistently less than 0.01. By using the paired t-test, at 0-year of age, it is found that the surface area of the left hemisphere is statistically (P < 0.001) larger than that of the right hemisphere, consistent to the report stating that the volume of the left hemisphere is larger than that of the right hemisphere at birth

(Gilmore et al. 2007), although no difference is found in hemispheric surface area due to small sample in (Hill, Dierker et al. 2010). However, no significant difference on the cortical surface areas between the left and right hemispheres has been found at 1 and 2 years of age, consistent to the findings on adults (Van Essen et al. 2011), where nearly same cortical surface areas of left versus right hemispheres are observed.

Table 2 provides the mean and standard deviation of the longitudinal cortical surface area expansion of the 73 subjects from 0 to 2 years of age. The surface area expansion is defined as the ratio of the later year central cortical surface area versus that of the earlier year. In the first year, the cortical surface area expands dramatically, with the average expansion around 1.80 times. By using paired t-test, it is found that the cortical surface area expansion of the right hemisphere is statistically (P < 0.001) larger than that of the left hemisphere from 0 to 1 year of age. This might explain the above findings: although the cortical surface area of the left hemisphere is statistically larger than that of the right hemisphere at 0 year of age, no significant difference between the cortical surface areas of left and right hemispheres exists at 1 year of age. In the second year, the cortical surface area expansion is still substantial, with the average expansion around 1.20 times. No significant difference on the cortical surface area expansion between the left and right hemispheres has been found from 1 to 2 years of age. Our results are consistent with the results in (Knickmeyer et al. 2008; Gilmore et al. 2011), where cortical gray matter volume growth is rapid in the first 2 years of life, especially in the first year. Although the cortical surface area of male is statistically larger than that of female in each hemisphere at each age, no significant difference in the cortical surface area expansion between male and female has been found from 0 to 1 year of age and from 1 to 2 years of age.

Longitudinal Surface-Based Atlases at 0, 1, and 2 Years of Age

Figure 3 shows the generated longitudinal surface-based atlases of cortical structures of the left hemisphere at 0, 1, and 2 years of age. Major cortical folding patterns are similar in terms of average convexity and mean curvature at 0, 1, and 2 years of age, suggesting that the shapes of major cortical folding of sulci and gyri have been well developed at term birth, which is consistent to the findings in (Hill, Dierker

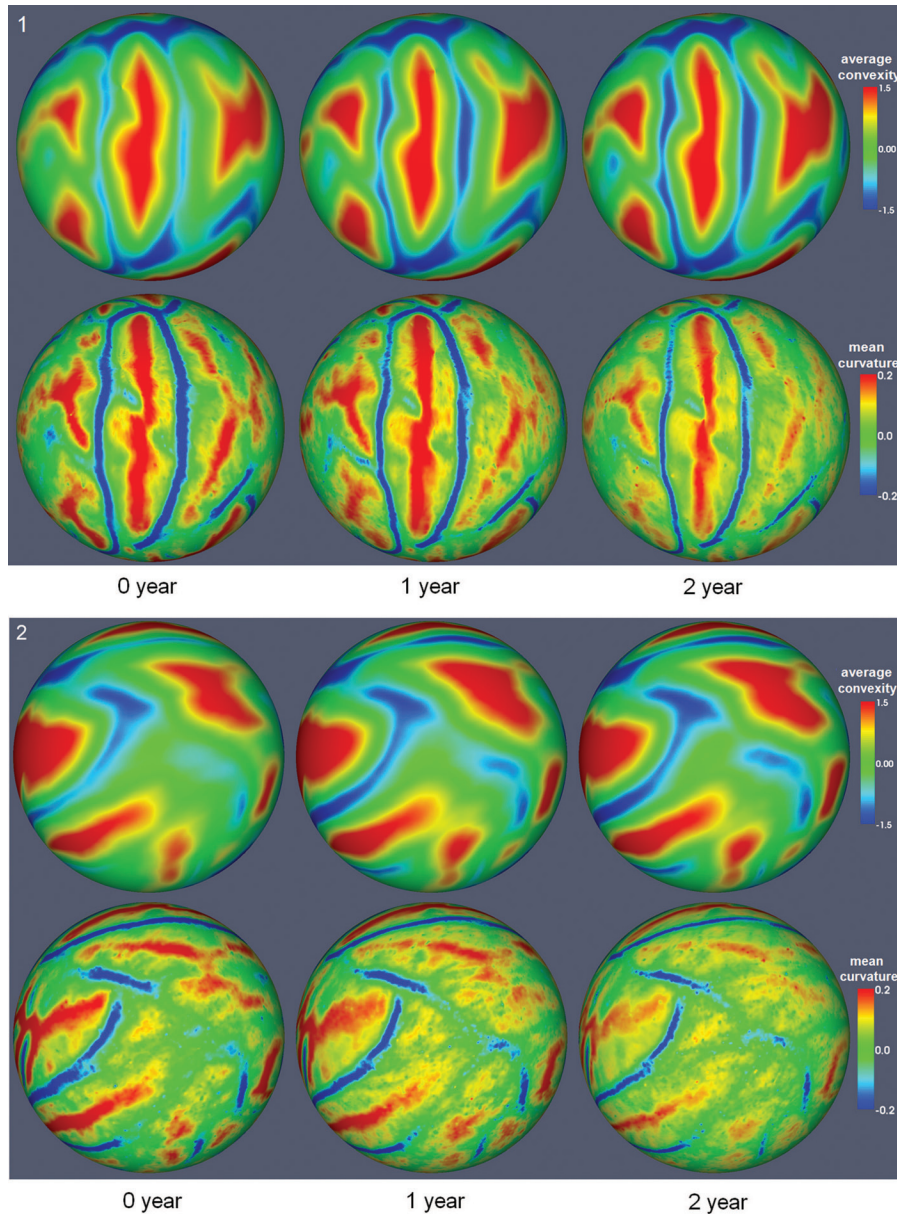| Subjects	0–1-year of age expansion		1–2-year old expansion		0–2-year old expansion	
	Left	Right	Left	Right	Left	Right
All (n = 73)	1.78 ± 0.16	1.81 ± 0.16	1.20 ± 0.05	1.20 ± 0.05	2.15 ± 0.18	2.18 ± 0.18
Male (n = 42)	1.76 ± 0.15	1.79 ± 0.15	1.22 ± 0.06	1.21 ± 0.06	2.13 ± 0.19	2.17 ± 0.19
Female (n = 31)	1.82 ± 0.17	1.84 ± 0.17	1.19 ± 0.05	1.19 ± 0.05	2.18 ± 0.18	2.19 ± 0.18

Figure 3. The longitudinal surface-based atlases of cortical structures of left hemisphere at 0, 1, and 2 years of age, reconstructed from 73 subjects. 3-1 and 3-2 show 2 different views.

et al. 2010), and are well preserved during cortical development from 0 to 2 years of age. However, some minor differences on the appearance of cortical folding can still be observed, such as the increasing trend of the magnitude of average convexity and the decreasing trend of the magnitude of mean curvature from 0 to 2 years of age. The same findings have also been observed on the right hemisphere.

Figure 4 shows the average central cortical surfaces of the 73 subjects at 0, 1, and 2 years of age, generated by averaging the 3D positions of corresponding vertices of all cortical surfaces after affine alignment to the age-matched infant image intensity atlas (Shi et al. 2011). In the first year, the average cortical surface expands dramatically, while, in the second year, the average cortical surface expands much less than the
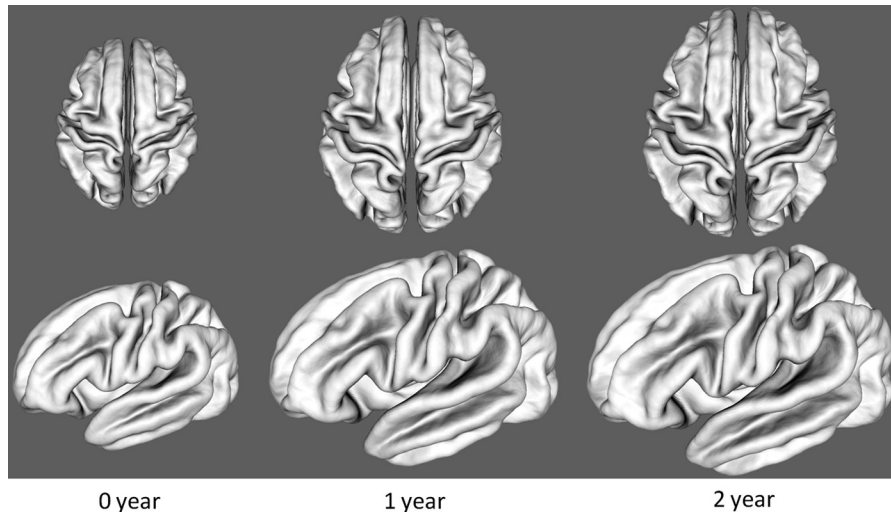
Figure 4. The average central cortical surfaces of the 73 subjects at 0, 1, and 2 years of age.

first year, although the expansion is still considerable. Meanwhile, the distance from the gyral crest to the sulcal bottom increases considerably from 0 to 2 years of age. However, the shapes of major cortical folding of sulci and gyri are quite similar at 0, 1, and 2 years of age, consistent with the above finding of cortical folding measurements of average convexity and mean curvature in Figure 3.

Region-Specific Surface Area Expansion in the First Year

Figure 5a shows the map of longitudinally cortical surface area expansion on both hemispheres from 0 to 1 year of age. Each region of the cortical surface increases in absolute surface area; however, the areal expansion is highly nonuniform across different cortical regions. In general, the areal expansions in the parietal, temporal, and occipital lobes are larger than those of the frontal lobes in both hemispheres. Specifically, high-expansion regions are concentrated in superior and medial temporal cortices, superior parietal cortices, medial orbitofrontal cortices, lateral anterior prefrontal cortices, occipital lobes, and postcentral gyri in both hemispheres. Low-expansion regions are concentrated in precentral gyri, superior frontal cortices, orbitofrontal cortices, cingulate cortices, precuneus regions, and insular regions in both hemispheres. By using *t*-tests with setting of significant level as $P = 0.01$ (corrected for multiple comparisons with 5000 iterations of permutation testing [Nichols and Holmes 2002]), the white contours in the Figure 5a enclose the cortical regions that expand significantly larger than the average expansion, whereas the black contours enclose the cortical regions that expand significantly smaller than the average expansion. In general, the regions passing significance are similar in the 2 hemispheres.

Region-Specific Surface Area Expansion in the Second Year

Figure 5b shows the map of longitudinally cortical surface area expansion from 1 to 2 years of age. Similar to the finding in the first year, each region of the cortical surface increases in absolute surface area, while the expansion is also highly nonuniform across different cortical regions. However, high-expansion and low-expansion regions from 1 to 2 years of age are quite different from those from 0 to 1 year of age. In general, the areal expansions in the parietal, temporal, and frontal lobes are larger than those of the occipital lobes in both hemispheres, consistent to the findings that the gray matter volumes of parietal lobes, frontal lobes, and temporal poles grow relatively fast (Gilmore et al. 2011) in the second year. Specifically, the high-expansion regions are concentrated in superior and middle frontal cortices, orbitofrontal cortices, inferior temporal cortices, inferior parietal cortices, superior parietal cortices, and isthmus of the cingulate cortex in both hemispheres. The low-expansion regions are concentrated in central sulci, paracentral lobules, superior temporal cortices, occipital lobes, and insular regions in both hemispheres. Similarly, the white (or black) contours enclose the cortical regions that expand significantly larger (or smaller) than the average areal expansion, respectively. In general, the regions passing significance are similar in both hemispheres.

Region-Specific Surface Area Expansion in the First 2 Years

Figure 5c shows the maps of longitudinally cortical surface area expansion from 0 to 2 years of age. The high-expansion regions are concentrated in anterior prefrontal cortices, medial orbitofrontal cortices, parietal cortices, lateral temporal cortices, cuneus cortices, and lingual cortices in both hemispheres. The low-expansion regions are concentrated in central sulci, precentral gyri, paracentral lobules, cingulate cortices, calcarine sulci, parieto-occipital sulci and insular regions in both hemispheres. Similarly, the white (or black) contours enclose the cortical regions that expand significantly larger (or smaller) than the average areal expansion, respectively.

Discussion

For the first time, we have quantitatively characterized the pattern of longitudinal cortical surface area expansion in the first 2 years of life by establishing the first longitudinal surface-based atlases of human cortical structures at 0, 1, and 2 years of age, which will facilitate the surface-based analysis of cortical folding and development in early postnatal stages of life. We find that major cortical folding of sulci and gyri
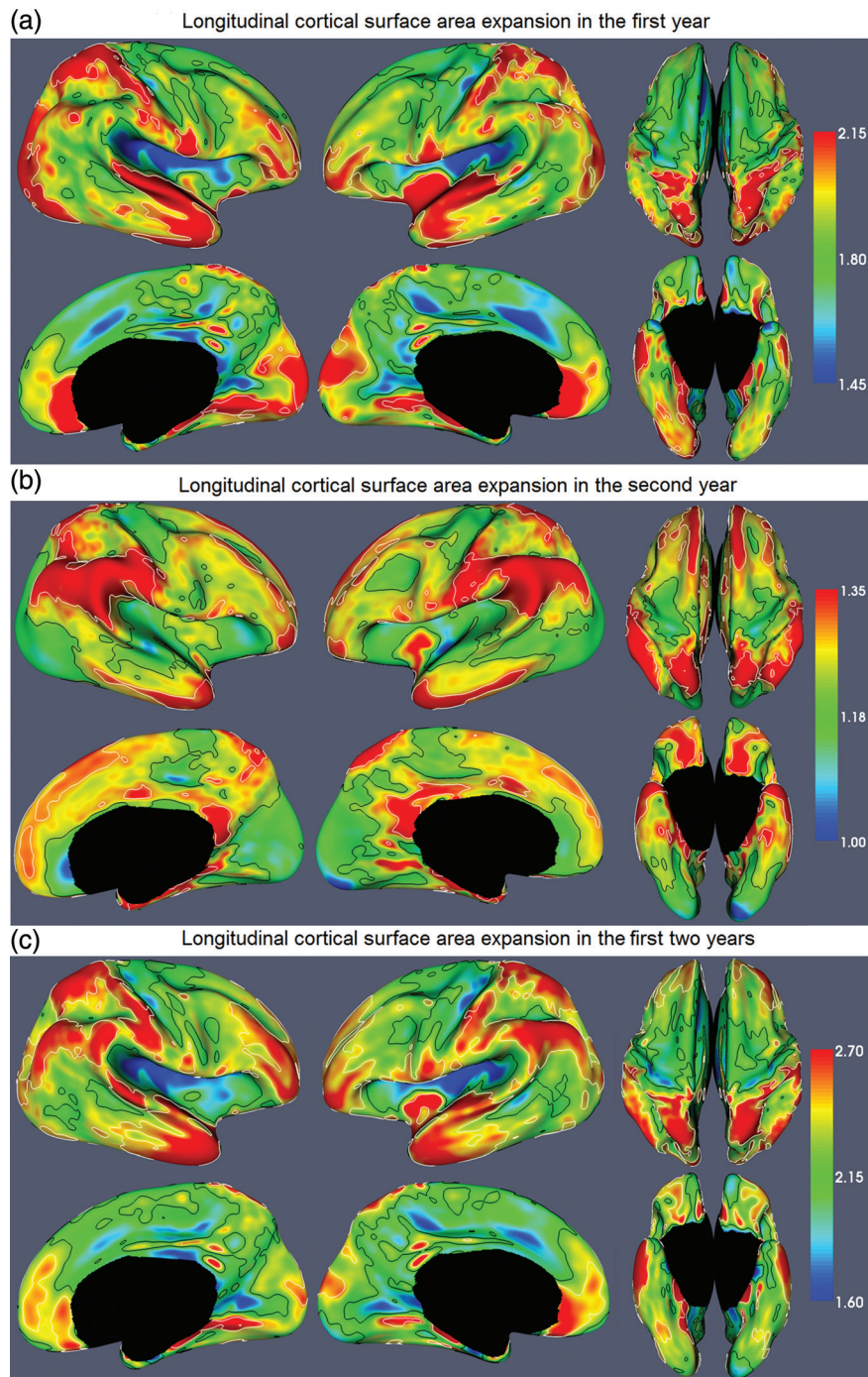
Figure 5. The maps of longitudinally cortical surface area expansion from 0 to 2 years of age. The color bar is shown on the right. The white and black contours enclose the cortical regions that expand significantly larger and smaller than the average areal expansion, respectively.

have been well developed at term birth, consistent with previous findings (Retzius 1890; Chi et al. 1977; Hill, Dierker et al. 2010), and are well preserved during cortical development from 0 to 2 years of age. Only the tertiary folding structures are still undergoing rapid development after birth. Therefore, the considerable variability of cortical folding across adult individuals is primarily established by term birth (Hill, Dierker et al. 2010). Cortical connectivity is thought as the major driving force of the cortical folding (Van Essen 1997; Nie, Guo et al. 2011), where consistent cortical folding is predicted to occur in regions with cortical connections dominated by few pathways between large areas (Van Essen 1997; Hill, Dierker et al. 2010). Since at term birth nearly every long-distance cortico-cortical and callosal connection has formed and only short cortico-cortical connections are still developing (Kostovic and Jovanov-Milosevic 2006; Takahashi et al. 2012), our result supports the hypothesis that cortical connectivity drives the variability of cortical folding (Van Essen 1997; Nie, Guo et al. 2011). Cortical folding abnormalities, which have been found in many neurodevelopmental disorders, such as autism (Nordahl et al. 2007), Williams syndrome (Van Essen et al. 2006), and bipolar disorder (Fornito

et al. 2007), might have origins at term birth. Therefore, studying the cortical folding and development of neonates with high risks of neurodevelopmental disorders would help understand these disorders.

We find that the cortical surface area expansion is age related and region specific. In the first year, the surface area expands 1.80 times and the high-expansion regions are concentrated in superior temporal (auditory cortex), superior parietal (involved with multisensory integration [Molholm et al. 2006]), medial orbitofrontal, and lateral anterior prefrontal cortices, as well as postcentral gyrus (primary somatosensory cortex) and occipital lobe (visual cortex). This pattern might reflect the rapid development of visual, auditory, and sensory functions relative to the motor and association areas in the first year. In the second year, the surface area expands 1.20 times and the high-expansion regions are concentrated in the superior frontal (involved with motor planning [Schilling et al. 2012]), middle frontal (involved with self-evaluation [Beer et al. 2010]), inferior temporal (involved with high-order visual processing, including shapes and faces [Denys et al. 2004; Sabatinelli et al. 2011]), superior parietal (involved with visuospatial and attentional processing (Nachev and Husain 2006)), orbitofrontal (involved with decision making [Kringelbach 2005]), and inferior parietal cortices (involved with receiving auditory, visual, and somatosensory inputs [Rozzi et al. 2008]).

Cortical neurogenesis and migration are completed by the first week of postnatal life (Rakic 2009; Clowry et al. 2010; Hill, Inder et al. 2010). After that, cortical development is largely dependent on dendritic growth, growth of the terminal axon arborization, myelination, and synaptogenesis (Flechsig et al. 1896; Mrzljak et al. 1990; Koenderink et al. 1994; Rakic et al. 1994; Koenderink and Uylings 1995; Petanjek et al. 2011). Dendritic outgrowth during the first 2 years might count more for changes in cortical volume (Petanjek et al. 2008). In prefrontal layer IIIC pyramidal neurons, the total number of dendritic segments reached adult levels at the age of 1 postnatal month, and the total length of basal dendritic tree increased 3 times from birth to 2.5 months, remained "dormant" between 2.5 and 16 months and increased again until 2.5 years (Petanjek et al. 2008). In prefrontal layer V pyramidal neurons, no new dendritic segments were elaborated after birth, and the values of dendritic length became close to adult values at 12–15 months, with the most intensive period of postnatal dendritic growth occurring during the first 3 postnatal months (Petanjek et al. 2008). The basic unit of the mature neocortex is the minicolumn, a narrow chain of neurons extending vertically across the cellular layers II–VI, perpendicular to the pial surface (Mountcastle 1997). At the end of gestation, the mean width of a minicolumn was about one-third adult size (Buxhoeveden and Casanova 2002), and the neurons are rarely generated after birth in the cerebral cortex (Rakic 1988). Therefore, the expansion of cortical surface area is likely caused by expansions of minicolumns.

Human brain is regionally highly differentiated but hierarchically and geometrically organized (Chen et al. 2012; Wedeen et al. 2012; Zilles and Amunts 2012). The cortical subdivision are nested in a common superstructure and interrelated in a tree-like organization, showing different degrees of functional, molecular, genetic, or structural similarities. The region-specific cortical surface areal expansion might relate to cellular, functional, and genetic nonuniformities during development. In general, high-expansion regions in

the first year tend to peak synaptic density (Huttenlocher and Dabholkar 1997), gray matter density (Gogtay et al. 2004), cortical thickness (Shaw et al. 2008), and functional maturation (Chugani and Phelps 1986; Chugani 1998) earlier than the high-expansion regions in the second year. The longitudinal regional variation of cortical surface area expansion supports the regional differences in synapse development in human brain development, with the synaptic density peaked at 3 months in the auditory cortex and at 3.5 years in the middle frontal gyrus (Huttenlocher and Dabholkar 1997). Similarly, the somatic sensory cortex (postcentral gyrus) and occipital pole peak cortical thickness earlier than high-order cortical areas, such as prefrontal and cingulate cortices (Shaw et al. 2008). And the sensorimotor cortex and occipital pole peak gray matter density earlier than the regions involved in executive function, attention, and motor coordination (prefrontal cortex) (Gogtay et al. 2004). Motor, visual, auditory, and somatosensory cortices are the early myelinating regions (Flechsig et al. 1896). In the first 3 postnatal months, glucose metabolic activity in PET increases more in the parietal, temporal, and primary visual cortices than the frontal cortex (Chugani and Phelps 1986; Chugani 1998). In the first 2 postnatal months, PET imaging or scalp recording can detect the activity in some high-expansion regions in the first year, including auditory cortex in response to sound and the medial temporal cortex in response to visually presented faces (de Haan and Nelson 1997; Tzourio-Mazoyer et al. 2002; Wakai et al. 2007; Hill, Inder et al. 2010). In contrast, transcranial magnetic stimulation of the motor cortex does not elicit detectable muscle response until 2 years of age (Nezu et al. 1997; Martin 2005; Hill, Inder et al. 2010). This longitudinal cortical surface area expansion pattern is also consistent with the cortical functional network development. For example, in infants, the resting-state networks are present in sensorimotor, visual, and auditory cortices (Fransson et al. 2007; Lin et al. 2008), with cortical hubs found in motor, sensory, auditory, and primary visual cortices (Fransson et al. 2011). However, the default network involving inferior parietal, prefrontal, and temporal cortices does not fully develop until 2 years of life (Gao et al. 2009).

In our previous study on longitudinal cortex development using the same set of samples, cortical gray matter volume was found to increase for 106% in the first year and 19% in the second year by using mixed models (Gilmore et al. 2011). While, in our current study, cortical surface area was found to expand for 80% (1.80 times) in the first year and 20% (1.20 times) in the second year. As the cortex volume is jointly characterized by cortical surface area and cortical thickness, the above findings might indicate that the cortical thickness may increase considerably in the first year, but is relatively unchanged in the second year, indicating the highly nonuniform developmental trajectories of cortical surface area and cortical thickness in the first 2 years. Moreover, the region-specific cortical surface area expansion pattern is more similar to the cortical volume growth pattern in the second year than that in the first year. For example, in the second year, the cortical volume grows relatively more rapidly in the parietal lobes, prefrontal cortices, and temporal poles (Gilmore et al. 2011), which are similar to the regions with larger cortical surface area expansion, suggesting that the cortical volume growth might be primarily contributed by cortical surface area expansion. In contrast, the rapid cortical volume growth regions are

unrelated to the regions with larger cortical surface area expansion in the first year, suggesting that the cortical volume growth is jointly contributed by both cortical surface area expansion and cortical thickness growth at this stage. These findings may have clinical implications for understanding abnormal cortical development in neurodevelopmental disorders. For example, autism is associated with overgrowth of cortical volume in the first 2 years of life (Schumann et al. 2010; Hazlett et al. 2011), which are primarily caused by the increase of the cortical surface area rather than the cortical thickness (Hazlett et al. 2011). Since the cortical surface area expansion in the first year is much larger than that of the second year, the cortical volume overgrowth in autism might occur more likely in the first year (Gilmore et al. 2011). By correlating the longitudinal cortical surface expansion patterns with the adult cortical thickness map (Fischl and Dale 2000), the high-expansion regions in the first year (i.e., postcentral gyrus, superior parietal cortex, and occipital cortex) tend to be relatively thin in adults. This correlation is imperfect with the noteworthy exceptions including high-expansion regions of superior temporal, lateral anterior prefrontal, and medial orbitofrontal cortices, which are relatively thick in adults. All these implications and questions need to be further confirmed and answered with a longitudinal study of cortical thickness development in the first 2 years of life.

Funding

Notes

Conflict of Interest: None declared.

References

Armstrong E, Schleicher A, Omran H, Curtis M, Zilles K. 1995. The ontogeny of human gyrification. Cereb Cortex. 5:56–63.

Beer JS, Lombardo MV, Bhanji JP. 2010. Roles of medial prefrontal cortex and orbitofrontal cortex in self-evaluation. J Cogn Neurosci. 22:2108–2119.

Buxhoeveden DP, Casanova MF. 2002. The minicolumn hypothesis in neuroscience. Brain. 125:935–951.

Chen CH, Gutierrez ED, Thompson W, Panizzon MS, Jernigan TL, Eyler LT, Fennema-Notestine C, Jak AJ, Neale MC, Franz CE et al. 2012. Hierarchical genetic organization of human cortical surface area. Science. 335:1634–1636.

Chi JG, Dooling EC, Gilles FH. 1977. Gyral development of the human brain. Ann Neurol. 1:86–93.

Chugani HT. 1998. A critical period of brain development: studies of cerebral glucose utilization with PET. Prev Med. 27:184–188.

Chugani HT, Phelps ME. 1986. Maturational changes in cerebral function in infants determined by 18FDG positron emission tomography. Science. 231:840–843.

Clowry G, Molnar Z, Rakic P. 2010. Renewed focus on the developing human neocortex. J Anat. 217:276–288.

de Haan M, Nelson CA. 1997. Recognition of the mother's face by six-month-old infants: a neurobehavioral study. Child Dev. 68:187–210.

Denys K, Vanduffel W, Fize D, Nelissen K, Peuskens H, Van Essen D, Orban GA. 2004. The processing of visual shape in the cerebral cortex of human and nonhuman primates: a functional magnetic resonance imaging study. J Neurosci. 24:2551–2565.

Dubois J, Benders M, Cachia A, Lazeyras F, Ha-Vinh Leuchter R, Sizonenko SV, Borradori-Tolsa C, Mangin JF, Huppi PS. 2008. Mapping the early cortical folding process in the preterm newborn brain. Cereb Cortex. 18:1444–1454.

Fischl B, Dale AM. 2000. Measuring the thickness of the human cerebral cortex from magnetic resonance images. Proc Natl Acad Sci U S A. 97:11050–11055.

Fischl B, Liu A, Dale AM. 2001. Automated manifold surgery: constructing geometrically accurate and topologically correct models of the human cerebral cortex. IEEE Trans Med Imaging. 20:70–80.

Fischl B, Sereno MI, Dale AM. 1999. Cortical surface-based analysis. II: Inflation, flattening, and a surface-based coordinate system. Neuroimage. 9:195–207.

Fischl B, Sereno MI, Tootell RB, Dale AM. 1999. High-resolution intersubject averaging and a coordinate system for the cortical surface. Hum Brain Mapp. 8:272–284.

Flechsig P, Eifrig D, Burian HM, Hermann M. Burian Ophthalmology Collection. 1896. Gehirn und seele: Rede, gehalten am 31. october 1894 in der Universitätskirche zu Leipzig. Leipzig: Veit & Co.

Fornito A, Malhi GS, Lagopoulos J, Ivanovski B, Wood SJ, Velakoulis D, Saling MM, McGorry PD, Pantelis C, Yucel M. 2007. In vivo evidence for early neurodevelopmental anomaly of the anterior cingulate cortex in bipolar disorder. Acta Psychiatr Scand. 116: 467–472.

Fransson P, Aden U, Blennow M, Lagercrantz H. 2011. The functional architecture of the infant brain as revealed by resting-state fMRI. Cereb Cortex. 21:145–154.

Fransson P, Skiold B, Horsch S, Nordell A, Blennow M, Lagercrantz H, Aden U. 2007. Resting-state networks in the infant brain. Proc Natl Acad Sci U S A. 104:15531–15536.

Gao W, Zhu H, Giovanello KS, Smith JK, Shen D, Gilmore JH, Lin W. 2009. Evidence on the emergence of the brain's default network from 2-week-old to 2-year-old healthy pediatric subjects. Proc Natl Acad Sci U S A. 106:6790–6795.

Gilmore JH, Lin W, Prastawa MW, Looney CB, Vetsa YS, Knickmeyer RC, Evans DD, Smith JK, Hamer RM, Lieberman JA et al. 2007. Regional gray matter growth, sexual dimorphism, and cerebral asymmetry in the neonatal brain. J Neurosci. 27:1255–1260.

Gilmore JH, Shi F, Woolson SL, Knickmeyer RC, Short SJ, Lin W, Zhu H, Hamer RM, Styner M, Shen D. 2011. Longitudinal development of cortical and subcortical gray matter from birth to 2 years. Cereb Cortex. In press.

Gogtay N, Giedd JN, Lusk L, Hayashi KM, Greenstein D, Vaituzis AC, Nugent TF 3rd, Herman DH, Clasen LS, Toga AW et al. 2004. Dynamic mapping of human cortical development during childhood through early adulthood. Proc Natl Acad Sci U S A. 101:8174–8179.

Han X, Jovicich J, Salat D, van der Kouwe A, Quinn B, Czanner S, Busa E, Pacheco J, Albert M, Killiany R et al. 2006. Reliability of MRI-derived measurements of human cerebral cortical thickness: the effects of field strength, scanner upgrade and manufacturer. Neuroimage. 32:180–194.

Hazlett HC, Poe MD, Gerig G, Styner M, Chappell C, Smith RG, Vachet C, Piven J. 2011. Early brain overgrowth in autism associated with an increase in cortical surface area before age 2 years. Arch Gen Psychiatry. 68:467–476.

Hill J, Dierker D, Neil J, Inder T, Knutsen A, Harwell J, Coalson T, Van Essen D. 2010. A surface-based analysis of hemispheric asymmetries and folding of cerebral cortex in term-born human infants. J Neurosci. 30:2268–2276.

Hill J, Inder T, Neil J, Dierker D, Harwell J, Van Essen D. 2010. Similar patterns of cortical expansion during human development and evolution. Proc Natl Acad Sci U S A. 107:13135–13140.

Huttenlocher PR, Dabholkar AS. 1997. Regional differences in synaptogenesis in human cerebral cortex. J Comp Neurol. 387:167–178.

Knickmeyer RC, Gouttard S, Kang C, Evans D, Wilber K, Smith JK, Hamer RM, Lin W, Gerig G, Gilmore JH. 2008. A structural MRI study of human brain development from birth to 2 years. J Neurosci. 28:12176–12182.

Koenderink MJ, Uylings HB. 1995. Postnatal maturation of layer V pyramidal neurons in the human prefrontal cortex. A quantitative Golgi analysis. Brain Res. 678:233–243.

Koenderink MJ, Uylings HB, Mrzljak L. 1994. Postnatal maturation of the layer III pyramidal neurons in the human prefrontal cortex: a quantitative Golgi analysis. Brain Res. 653:173–182.

Kostovic I, Jovanov-Milosevic N. 2006. The development of cerebral connections during the first 20–45 weeks' gestation. Semin Fetal Neonatal Med. 11:415–422.

Kringelbach ML. 2005. The human orbitofrontal cortex: linking reward to hedonic experience. Nat Rev Neurosci. 6:691–702.

Li G, Nie J, Wu G, Wang Y, Shen D. 2012. Consistent reconstruction of cortical surfaces from longitudinal brain MR images. Neuroimage. 59:3805–3820.

Lin W, Zhu Q, Gao W, Chen Y, Toh CH, Styner M, Gerig G, Smith JK, Biswal B, Gilmore JH. 2008. Functional connectivity MR imaging reveals cortical functional connectivity in the developing brain. AJNR Am J Neuroradiol. 29:1883–1889.

Liu T, Nie J, Tarokh A, Guo L, Wong ST. 2008. Reconstruction of central cortical surface from brain MRI images: method and application. Neuroimage. 40:991–1002.

Martin JH. 2005. The corticospinal system: from development to motor control. Neuroscientist. 11:161–173.

Molholm S, Sehatpour P, Mehta AD, Shpaner M, Gomez-Ramirez M, Ortigue S, Dyke JP, Schwartz TH, Foxe JJ. 2006. Audio-visual multisensory integration in superior parietal lobule revealed by human intracranial recordings. J Neurophysiol. 96:721–729.

Mountcastle VB. 1997. The columnar organization of the neocortex. Brain. 120(Pt 4):701–722.

Mrzljak L, Uylings HB, Van Eden CG, Judas M. 1990. Neuronal development in human prefrontal cortex in prenatal and postnatal stages. Prog Brain Res. 85:185–222.

Nachev P, Husain M. 2006. Disorders of visual attention and the posterior parietal cortex. Cortex. 42:766–773.

Nezu A, Kimura S, Uehara S, Kobayashi T, Tanaka M, Saito K. 1997. Magnetic stimulation of motor cortex in children: maturity of corticospinal pathway and problem of clinical application. Brain Dev. 19:176–180.

Nichols TE, Holmes AP. 2002. Nonparametric permutation tests for functional neuroimaging: a primer with examples. Hum Brain Mapp. 15:1–25.

Nie J, Guo L, Li K, Wang Y, Chen G, Li L, Chen H, Deng F, Jiang X, Zhang T et al. 2011. Axonal fiber terminations concentrate on gyri. Cereb Cortex. In press.

Nie J, Li G, Wang L, Gilmore JH, Lin W, Shen D. 2011. A computational growth model for measuring dynamic cortical development in the first year of life. Cereb Cortex. In press.

Nordahl CW, Dierker D, Mostafavi I, Schumann CM, Rivera SM, Amaral DG, Van Essen DC. 2007. Cortical folding abnormalities in autism revealed by surface-based morphometry. J Neurosci. 27:11725–11735.

Ono M, Kubik S, Abernathey CD. 1990. Atlas of the cerebral sulci. G. Thieme Medical Publishers: New York.

Petanjek Z, Judas M, Kostovic I, Uylings HB. 2008. Lifespan alterations of basal dendritic trees of pyramidal neurons in the human prefrontal cortex: a layer-specific pattern. Cereb Cortex. 18:915–929.

Petanjek Z, Judas M, Simic G, Rasin MR, Uylings HB, Rakic P, Kostovic I. 2011. Extraordinary neoteny of synaptic spines in the human prefrontal cortex. Proc Natl Acad Sci U S A. 108:13281–13286.

Rakic P. 2009. Evolution of the neocortex: a perspective from developmental biology. Nat Rev Neurosci. 10:724–735.

Rakic P. 1988. Specification of cerebral cortical areas. Science. 241:170–176.

Rakic P, Bourgeois JP, Goldman-Rakic PS. 1994. Synaptic development of the cerebral cortex: implications for learning, memory, and mental illness. Prog Brain Res. 102:227–243.

Retzius MG. 1890. Biologische Untersuchungen … Neue Folge (Illustrated). Samson & Wallin: Stockholm.

Rozzi S, Ferrari PF, Bonini L, Rizzolatti G, Fogassi L. 2008. Functional organization of inferior parietal lobule convexity in the macaque monkey: electrophysiological characterization of motor, sensory and mirror responses and their correlation with cytoarchitectonic areas. Eur J Neurosci. 28:1569–1588.

Sabatinelli D, Fortune EE, Li Q, Siddiqui A, Krafft C, Oliver WT, Beck S, Jeffries J. 2011. Emotional perception: meta-analyses of face and natural scene processing. Neuroimage. 54:2524–2533.

Schilling C, Kuhn S, Paus T, Romanowski A, Banaschewski T, Barbot A, Barker GJ, Bruhl R, Buchel C, Conrod PJ et al. 2012. Cortical thickness of superior frontal cortex predicts impulsiveness and perceptual reasoning in adolescence. Mol Psychiatry. In press.

Schumann CM, Bloss CS, Barnes CC, Wideman GM, Carper RA, Akshoomoff N, Pierce K, Hagler D, Schork N, Lord C et al. 2010. Longitudinal magnetic resonance imaging study of cortical development through early childhood in autism. J Neurosci. 30:4419–4427.

Shattuck DW, Leahy RM. 2002. BrainSuite: an automated cortical surface identification tool. Med Image Anal. 6:129–142.

Shaw P, Kabani NJ, Lerch JP, Eckstrand K, Lenroot R, Gogtay N, Greenstein D, Clasen L, Evans A, Rapoport JL et al. 2008. Neurodevelopmental trajectories of the human cerebral cortex. J Neurosci. 28:3586–3594.

Shen D, Davatzikos C. 2004. Measuring temporal morphological changes robustly in brain MR images via 4-dimensional template warping. Neuroimage. 21:1508–1517.

Shi F, Wang L, Dai Y, Gilmore JH, Lin W, Shen D. 2012. LABEL: pediatric brain extraction using learning-based meta-algorithm. Neuroimage. 62:1975–1986.

Shi F, Yap PT, Wu G, Jia H, Gilmore JH, Lin W, Shen D. 2011. Infant brain atlases from neonates to 1- and 2-year-olds. PLoS One. 6: e18746.

Sled JG, Zijdenbos AP, Evans AC. 1998. A nonparametric method for automatic correction of intensity nonuniformity in MRI data. IEEE Trans Med Imaging. 17:87–97.

Takahashi E, Folkerth RD, Galaburda AM, Grant PE. 2012. Emerging cerebral connectivity in the human fetal brain: an MR tractography study. Cereb Cortex. 22:455–464.

Thompson DK, Warfield SK, Carlin JB, Pavlovic M, Wang HX, Bear M, Kean MJ, Doyle LW, Egan GF, Inder TE. 2007. Perinatal risk factors altering regional brain structure in the preterm infant. Brain. 130:667–677.

Toro R, Burnod Y. 2005. A morphogenetic model for the development of cortical convolutions. Cereb Cortex. 15:1900–1913.

Tzourio-Mazoyer N, De Schonen S, Crivello F, Reutter B, Aujard Y, Mazoyer B. 2002. Neural correlates of woman face processing by 2-month-old infants. Neuroimage. 15:454–461.

Van Essen DC. 2005. A population-average, landmark- and surface-based (PALS) atlas of human cerebral cortex. Neuroimage. 28:635–662.

Van Essen DC. 1997. A tension-based theory of morphogenesis and compact wiring in the central nervous system. Nature. 385:313–318.

Van Essen DC, Dierker D, Snyder AZ, Raichle ME, Reiss AL, Korenberg J. 2006. Symmetry of cortical folding abnormalities in Williams syndrome revealed by surface-based analyses. J Neurosci. 26:5470–5483.

Van Essen DC, Glasser MF, Dierker DL, Harwell J, Coalson T. 2011. Parcellations and hemispheric asymmetries of human cerebral cortex analyzed on surface-based atlases. Cereb Cortex. In press.

Wakai RT, Lutter WJ, Chen M, Maier MM. 2007. On and off magnetic auditory evoked responses in early infancy: a possible marker of brain immaturity. Clin Neurophysiol. 118:1480–1487.

Wang L, Shi F, Yap PT, Lin W, Gilmore JH, Shen D. 2011. Longitudinally guided level sets for consistent tissue segmentation of neonates. Hum Brain Mapp. In press.

Wedeen VJ, Rosene DL, Wang R, Dai G, Mortazavi F, Hagmann P, Kaas JH, Tseng WY. 2012. The geometric structure of the brain fiber pathways. Science. 335:1628–1634.

Xu C, Pham DL, Rettmann ME, Yu DN, Prince JL. 1999. Reconstruction of the human cerebral cortex from magnetic resonance images. IEEE Trans Med Imaging. 18:467–480.

Xue Z, Shen D, Davatzikos C. 2006. CLASSIC: consistent longitudinal alignment and segmentation for serial image computing. Neuroimage. 30:388–399.